International Journal of Science and Research (IJSR)
ISSN: 2319-7064
ResearchGate Impact Factor (2018): 0.28 | SJIF (2018): 7.426

Effect of Porous Layer on the Condensation of Falling Liquid Film on a Vertical Channel

Ashraf Noor Shafie[1], Husni Marwan Sharaf[2], Abdullah Manea Al-Batati[3], Abdelaziz Nasr[4]

Mechanical Engineering Department, College of Engineering, Umm Al-Qura University, Makkah P.O. BOX 5555, Kingdom of Saudi Arabia

Abstract: ***In this paper, we numerically investigate the condensation of water liquid film. The results concern the effects of porosity and porous layer thickness of the porous media on the heat and mass transfer performance and on the liquid condensation rate. It is shown that the presence of the porous layer improves the heat and mass transfer at the liquid-gas interface during the water liquid film condensation.***

Keywords: film evaporation, porous medium, mixed convection

1. Introduction

Heat and mass transfer during liquid film evaporation have been the subjects of recent research because of their various industrial applications such as in desalination, in distillation, in drying, cooling towers and air conditioning.

Debissi et al. [1] presented a numerical study of the evaporation of binary liquid film. The film falls down on one plate of a vertical channel under mixed convection. The first plate of a vertical channel is externally submitted to a uniform heated flux while the second is dry and isothermal. The liquid mixture consists of water (the more volatile component) and ethylene glycol while the gas mixture has three components: dry air, water vapour and ethylene-glycol vapour. They showed that from a definite distance and from a certain value of the inlet liquid mass fraction of ethylene glycol, it is possible to evaporate in the same conditions more water than if the film at the entry was pure water only. They showed that the existence and the value of the inversion distance essentially depend on the value of the heat flux density. Ben Jabrallah et al. [2] presented a numerical study of convective heat and mass transfer with evaporation of a falling film in a cavity. El Armouzi et al. [3] numerically studied the binary liquid film evaporation by mixed convection flowing down of two coaxial cylinders. They showed that the latent heat flux is the dominant mode for the present study. They also showed that the mass and heat transfers are more important near the inlet of the channel and increase with the wall heat flux density. Lazarus et al. [4] experimentally studied the steady state convective heat transfer of de-ionized water with a low volume fraction of copper oxide nanoparticles dispersed to form a nanofluid that flows through a copper tube. Agunaoun et al. [5] presented a numerical analysis of the heat and mass transfer in a binary liquid film flowing on an inclined plate. They showed that it is possible to increase the cumulated evaporation rate of water when the inlet liquid concentration of ethylene glycol is less than 40%. Recently, a new generation of coolant called nanofluids is used to improve heat transfer of liquids.

Khalal et al. [6] reported a numerical study of the heat and mass transfer during evaporation of a turbulent binary liquid film. They showed that the heat transferred through the latent mode is more pronounced when the concentration of volatile components is higher in the liquid mixture. Oubella et al. [7] studied numerically the heat and mass transfer with film evaporation in a vertical channel. They showed that the influence of the latent Nusselt numbers on the cooling of induced flows by evaporation depend largely on the inlet temperature and Reynolds number Re. They also showed that the better mass transfer rates related with film evaporation are found for a system with low mass diffusion coefficient. Nasr et al. [8] studied the evaporation of falling liquid film on one of two vertical plates covered with a thin porous layer by free convection.

The objective of this work is therefore to study the effect of the addition of different types of nanoparticles into water on the heat and mass transfer performance and on the water film evaporation.

2. Analysis

This work presents a numerical study of evaporation by mixed convection of a liquid film following on one of two vertical parallel plates (Fig.1). The film is a water-based nanofluid liquid, containing nanoparticles of aluminium. The wetted plate is externally subjected to a uniform heated flux or adiabatic while the second one is dry and isothermal. The nanofluid film flows down with an inlet temperature T_{0L}, an inlet mass flow rate m_{L0} and a volume fraction of nanoparticles φ_0. The air enters the channel with a temperature T_0, a water vapour concentration c_0, a constant velocity u_0 and an ambient pressure p_0.

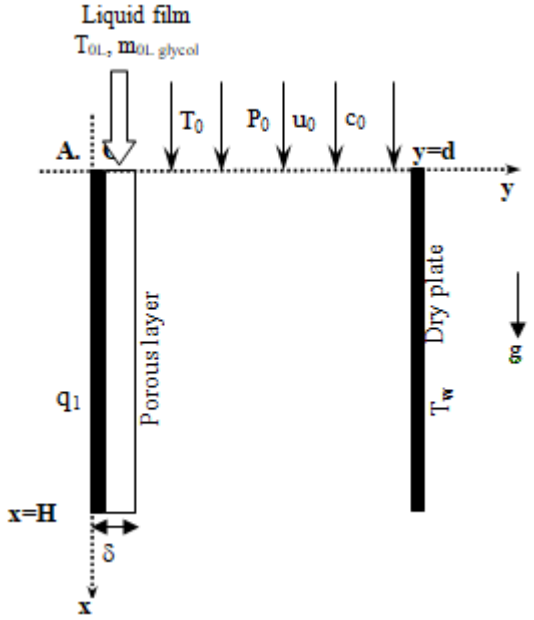

Figure 1: Physical System

2.1 Assumptions

For mathematical formulation of the problem, the following simplifying assumptions are introduced:

- Vapour mixture is ideal gas.
- The base fluid and the nanoparticles are in thermal equilibrium and no slip occurring between them.
- The liquid-gas interface is assumed impermeable to nanoparticles since the axial dynamic forces are much bigger then transversal forces
- The boundary layer approximations are used.
- Dufour and Soret effects are negligible.
- Flows and transfers in the two phases are steady, laminar and two dimensional.
- The effect of the superficial tension is negligible. The gas-liquid interface is in thermodynamic equilibrium.

2.2. Governing equations

Under the assumptions presented above, the equations governing the flow and the combined heat and mass transfers during water film evaporation in the liquid and in the gas phases are [8-10] as will be shown in the following subsections.

2.2.1. For the liquid phase

Continuity equation

$$\frac{\partial \rho_L u_L}{\partial x_L} + \frac{\partial \rho_L v_L}{\partial y_L} = 0$$

x-momentum equation

$$\rho_L g + \frac{\mu_L}{\varepsilon}\frac{\partial^2 u_L}{\partial y_L^2} - \frac{\mu_L}{K} u_L - \frac{\rho_L C}{\sqrt{K}} u_L^2 = 0$$

Energy equation

$$u_L \frac{\partial T_L}{\partial x_L} + v_L \frac{\partial T_L}{\partial y_L} = \alpha_e \frac{\partial^2 T_L}{\partial y_L^2}$$

2.2.2. For the gaseous phase

Continuity equation

$$\frac{\partial \rho u}{\partial x} + \frac{\partial \rho v}{\partial y} = 0$$

x-momentum equation

$$u\frac{\partial u}{\partial x} + v\frac{\partial u}{\partial y} = -\frac{1}{\rho}\frac{dP}{dx} - \beta g(T - T_0) - \beta^* g(c - c_0) + \frac{1}{\rho}\frac{\partial}{\partial y}\left(\mu \frac{\partial u}{\partial y}\right)$$

Energy equation

$$u\frac{\partial T}{\partial x} + v\frac{\partial T}{\partial y} = \frac{1}{\rho c_p}\left(\frac{\partial}{\partial y}\left(\lambda \frac{\partial T}{\partial y}\right) + \rho D\,(c_{pv} - c_{pa})\frac{\partial T}{\partial y}\frac{\partial c}{\partial y}\right)$$

Species diffusion equation

$$u\frac{\partial c}{\partial x} + v\frac{\partial c}{\partial y} = \frac{1}{\rho}\frac{\partial}{\partial y}\left(\rho D \frac{\partial c}{\partial y}\right)$$

The overall mass balance described by the following equation should be satisfied at every axial location:

$$\int_{\delta}^{d} \rho u dy = (d - \delta)\rho_0 u_0 - \int_0^x \rho v(x,0) dx$$

2.3 Boundary conditions

For inlet conditions (at x=0) :

T (0, y)=T_0; c(0, y)=c_0; u=u_0 and P=P_0

T_L (0, y_L)=T_{0L} ; $m(0, y_L) = m_{0L}$

For dry plate (at x=d) :

u(d, y) =0; v (d, y)= 0; $\left.\frac{\partial c}{\partial y}\right)_{x=d} = 0$ **; T(d, y)=T_w**

For wet plate (at y_L = 0) :

$$u_L(x,0) = v_L(x,0) = 0\,;\ q_w = -\lambda_{nf}\left.\frac{\partial T_{nf}}{\partial y_L}\right)_{y_L=0}\ ;$$

For gas-liquid interface (at y=0 and y_L =δ)

The continuities of the velocities and temperatures give:

$u_L(x, y_L = \delta) = u(x, y = 0)$; $T_L(x, y_L = 0) = T(x, y=0)$

The transverse velocity component of the mixture at the interface is obtained by assuming the interface to be semi-permeable:

$$v(x,0) = -\left.\frac{D}{1 - c(x,0)}\frac{\partial c}{\partial y}\right)_{y=0} \quad \text{where} \quad c(x,0) = c_{sat}(T(x,0))$$

$$c_{sat}(T(x,0)) = \frac{M_v}{M_g}\frac{P_{v,i}}{P_g}$$ where $p_{v,i}$ is the partial pressure of saturated vapour at the gas-liquid interface.

The continuities of shear stress give :

$$\left.\mu_{nf}\frac{\partial u_{nf}}{\partial y_L}\right)_{y_L=\delta} = \left.\mu\frac{\partial u}{\partial y}\right)_{y=0}$$

The heat balance at the interface implies:

$$-\lambda_{nf}\frac{\partial T_{nf}}{\partial y_L}\Big)_{y_L=\delta} = -\lambda\frac{\partial T}{\partial y}\Big)_{y=0} - \frac{\rho L_v D}{1-c(x,0)}\frac{\partial c}{\partial y}\Big)_{y=0}$$

where L_v is the latent heat of water evaporation

In order to evaluate the importance of the different processes of energy transfer, the following quantities are introduced.

The local condensation rate of water at the interface is given by:

$$\dot{m}(x) = -\frac{\rho D}{1-c(x,0)}\frac{\partial c}{\partial y}\Big)_{y=0}$$

The cumulated condensation rate of water at the interface is given by:

$$Mr(x) = \int_0^x \dot{m}(x)dx$$

3. Solution Method

The system of equations in the liquid and in the gaseous phases (1–8) and their boundary conditions given by Eqs (9-16) are solved numerically using a finite difference method. The flow area is divided into a regular mesh placed in axial and transverse direction and a 51x21x31 grid is retained in actual computations. A fully implicit marching scheme where the axial convection terms were approximated by the upstream difference and the transverse convection and diffusion terms by the central difference is employed to transform the governing equations into finite difference equations.

4. Results and Discussion

Fig.2 illustrates the evolution of the temperature and the vapor concentration at the liquid-vapor interface for various porosity ε. It is shown from fig.2a that an increase of porosity enhances the cooling at the interface. This result has been explained by the fact that the presence of the porous layer increases the heat transfer area of the liquid film and lets heat more effectively transfer to the liquid film. Fig.2b indicates that the vapor concentration at the liquid-vapor interface decreases with an increase of the porosity ε. This result has been justified by the fact that the axial distributions of vapour concentration at the interface follow the same tendency as the temperature at the interface shown in Fig.2a, due to a lower temperature which results in a lower vapour concentration. Fig.3 gives the effect of porosity on the condensation rate of water.

Fig. 4 presents the effect of the porous layer thickness δ on the temperature and the vapor concentration at the liquid-vapor interface. The results from figure 4 indicate that the temperature (fig.4a) and the vapor concentration (fig.4b) at the liquid-vapor interface are reduced for thicker porous layer thickness. This result has been explained by the fact that the presence of the thicker porous layer prevents the heat transfer to the liquid film (fig.4a). It is observed from fig.5 that the film condensation rate increases as the porous layer thickness increases.

5. Conclusion

The condensation of water film flowing along one of the channel vertical plates has been numerically studied. A thin porous layer of thickness δ is covered on the wetted plate. The effects of porosity and porous layer thickness on the heat and mass transfer performance and on the water evaporation has been presented and analysed.

A brief summary of the major results is as follows:

1) A decrease of the porosity ε and of the porous layer thickness δ enhances the heat and mass transfer performances across the liquid-vapor interface.
2) The increase of the porosity ε improves the water film condensation.
3) An increase of porous layer thickness δ enhances the water film condensation.
4) The decrease of the cooling heat flux or the increase of the inlet gas and liquid temperature reduces the water film condensation.

References

[1] C. Debbissi Hfaiedh, A. Nasr and S. Ben Nasrallah, Numerical study of evaporation by mixed convection of a binary liquid film flowing down the wall of two vertical plates, Int. J. Thermal sciences 72 (2013) 34-46.
[2] S. Ben Jabrallah, A. Belghith, J.P. Corriou, Convective heat and mass transfer with evaporation of a falling film in a cavity, International Journal of Thermal Sciences 45 (2006) 16-28.
[3] M. El Armouzi. Etude numérique de l'évaporation en convection mixte d'un film liquide binaire ruisselant sur l'une des parois de deux cylindres coaxiaux. Thèse de l'Université de Perpignan 2000.
[4] L. G. Asirvatham, N. Vishal, S. K. Gangatharan, D. M. Lal. Experimental study on forced convective heat transfer with low volume fraction of CuO/water nanofluid. Energies; 2009; 2: 97-119.
[5] A. Agunaoun, A. Il Idrissi, A. Daif, R. Barriol, Etude de l'évaporation en convection mixtes d'un film liquide d'un mélange binaire s'écoulant sur un plan incliné soumis à un flux de chaleur constant. International Journal of Heat and Mass Transfer 41 (1998) pp. 2197-2210.
[6] Khalal, L., Feddaoui, M., Mediouni, T., Numerical study of heat and mass transfer during evaporation of a turbulent binary liquid film. Thermal science, International Scientific Journal, 2013, doi : 10.2298/TSCI120927025K.
[7] Oubella, M., Feddaoui, M., Mir, R., Numerical study of heat and mass transfer during evaporation of a thin liquid film" Thermal Sciences, International Scientific Journal., 2013, doi: 10.2298/TSCI130128145O.
[8] Abdelaziz Nasr, Abdulmajeed S. Al-Ghamdi, Numerical study of evaporation of falling liquid film on one of two vertical plates covered with a thin porous layer by free

convection, International Journal of Thermal Sciences 112 (2017) 335-344.
[9] W.M. Yan, T.F. Lin, Combined heat and mass transfer in natural convection between vertical parallel plates with film evaporation, Int. J. Heat Mass Transfer 33 (3) (1990) 529–541.
[10] W.M. Yan, C.Y. Soong, Convective heat and mass transfer along an inclined heated plate with film evaporation, Int. J. Heat Mass Transfer 38 (7) (1995) 1261-1269.

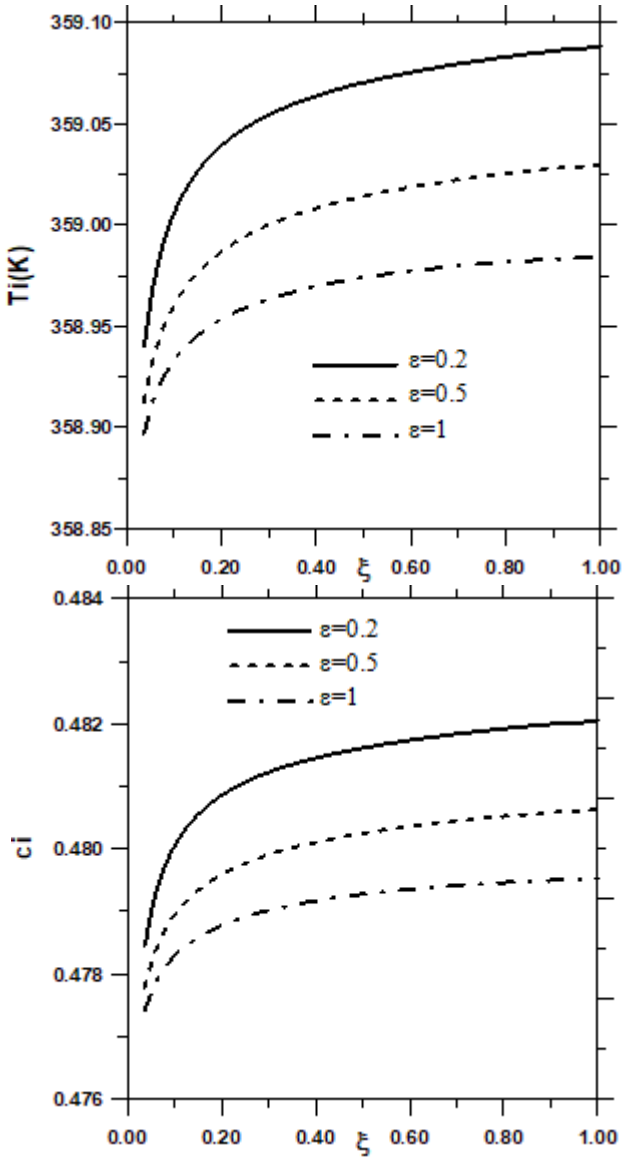

Figure 2: Variation of the vapor temperature (a) and concentration (b) at the liquid-vapor interface for various porosity ε: δ=0.001m, c_0=0.5, T0=293.15K, T0L=293.15K, Tw=293.15K, m_{0L}=0.001Kg/m.s, p_0=1 atm, q_1=0

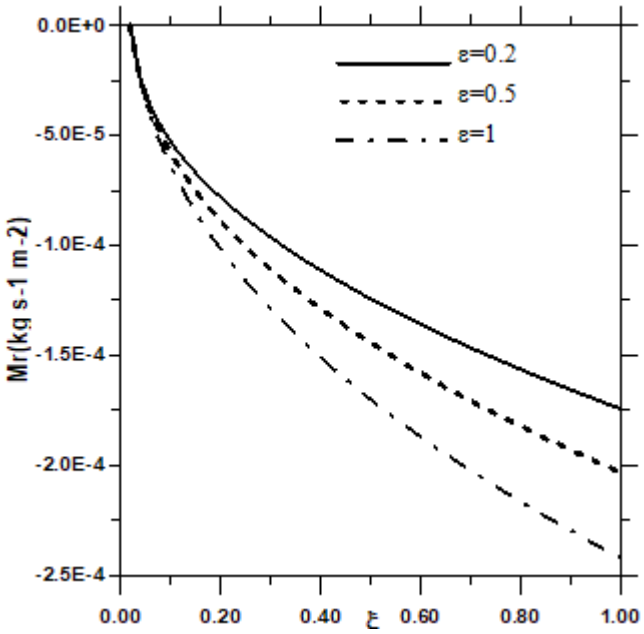

Figure 3: The evolution of the cumulated condensation rate of water for different values of porosity ε: δ=0.001m, c_0=0.5, T_0=293.15K, T_{0L}=293.15K, T_w=293.15K, m_{0L}=0.001Kg/m.s, p_0=1 atm, q_1=0

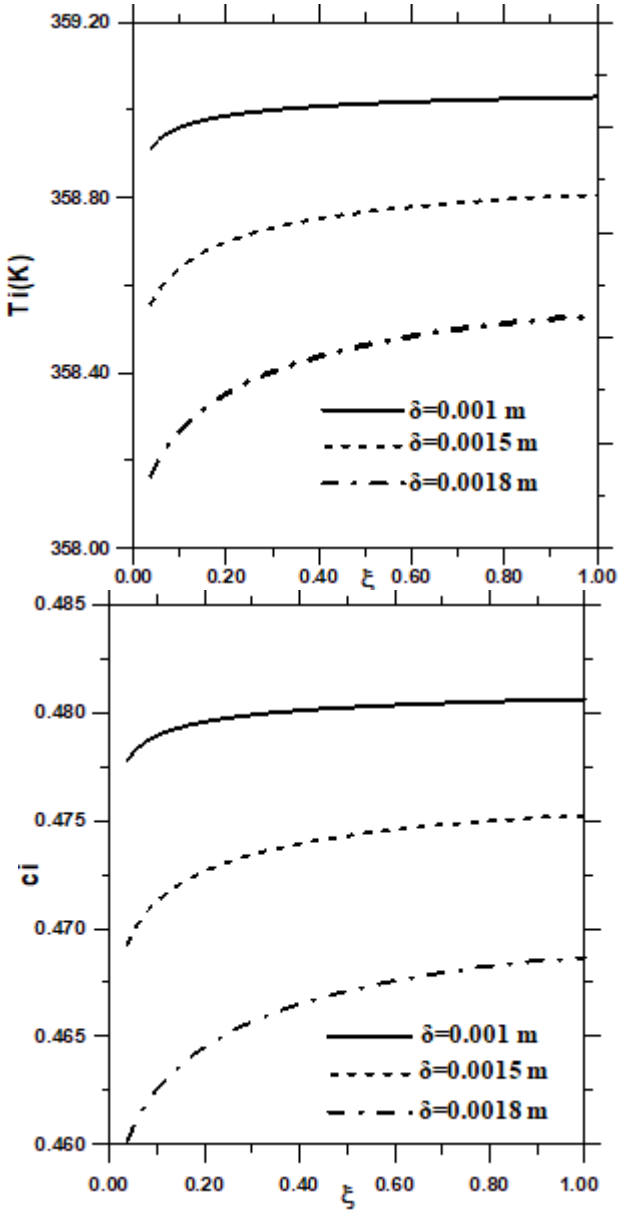

Figure 4: Variation of the vapor temperature (a) and concentration (b) at the liquid-vapor interface for various porous layer thickness δ : ε=0.5, c_0=0.5, T0=293.15K, T0L=293.15K, Tw=293.15K, m_{0L}=0.001Kg/m.s, p_0=1 atm, q_1=0

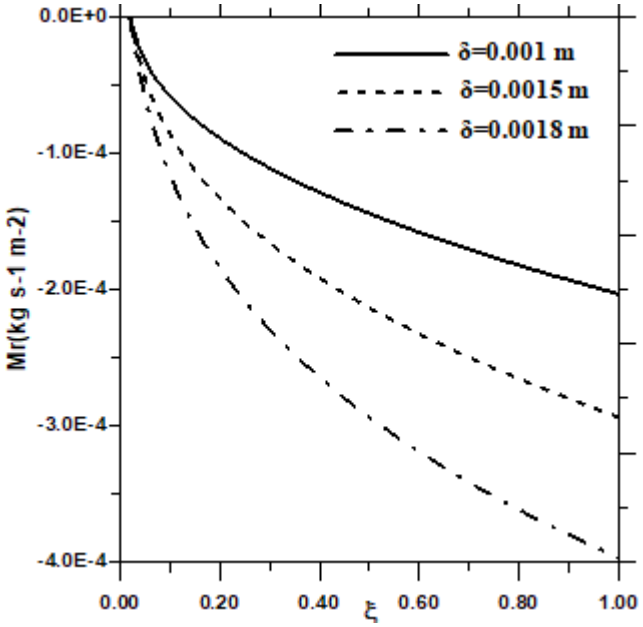

Figure 5: The evolution of the cumulated condensation rate of water for different values porous layer thickness δ: ε=0.5, c_0=0.5, T_0=293.15K, T_{0L}=293.15K, T_w=293.15K, m_{0L}=0.001Kg/m.s, p_0=1 atm, q_1=0